



Machining and environmental effects of electrostatic atomization lubrication in milling operation

Yu Su¹ · Qiong Lu¹ · Tong Yu¹ · Zhiqiang Liu¹ · Chunyan Zhang¹

Received: 27 December 2018 / Accepted: 9 July 2019 / Published online: 24 July 2019
© Springer-Verlag London Ltd., part of Springer Nature 2019

Abstract

The disadvantages of minimum quantity lubrication (MQL) are its poor cooling capability and environment and health hazard as a result of mist formation, resulting in considerable limitations on its widespread application. There is an urgent need to improve its cooling/lubrication performance and environmental performance. Electrostatic atomization is a method where the liquid is electrostatically charged and broken into fine charged droplets by means of electrical forces. This paper investigated the role of electrostatic atomization lubrication (EAL) and nanofluid electrostatic atomization lubrication (NFEAL) on tool wear in end milling of Ti-6Al-4V alloy, and evaluated their environmental performance in non-machining experiments in terms of oil mist concentrations of PM10 and PM2.5. For this research, electrostatic atomization milling system was designed and fabricated. A comparison with the results obtained under MQL condition is also provided. The experimental results show that there was a considerable reduction in tool wear and oil mist concentration for EAL and NFEAL as compared with MQL condition. Furthermore, NFEAL was more effective than EAL for reducing tool wear. But NFEAL yielded slightly higher oil mist concentration than EAL. Therefore, EAL and NFEAL seem to be potential cooling/lubricating approaches for the machining substituting MQL from view point of machining performance, health, and environment.

Keywords Electrostatic atomization lubrication · Minimum quantity lubrication · Tool wear · Oil mist concentration · Ti-6Al-4V

1 Introduction

Minimum quantity lubrication (MQL) is a method in which a minute quantity amount of lubricating oil is mixed with compressed air to form aerosol and sprayed into the machining zone for cooling and lubrication. MQL not only reduces the consumption rate of lubricating oil, but also results in the reduction of tool wear and improvement of surface quality in different material removal processes [1, 2]. However, there are two problems that limit the extensive use of MQL. One is its poor cooling capability and the other is air pollution and health hazards as a result of the production of mist [3, 4]. In MQL process, the cooling effect is provided by the convective heat transfer of compressed air and the evaporation of lubricating oil. Due to the low thermal capacity of air and lubricating oil, the cooling capacity of MQL is insufficient for the cutting

operation with excessive heat generation. In addition, when spraying air-oil mixture during MQL, mist is dispersed in the surrounding environment, which leads to air pollution and health hazards for workers. The Cincinnati University and Techsolve, Inc. jointly studied the concentration of oil mist particles in air under MQL and flood cooling conditions. It was found that at low cutting speed and metal removal rate, the oil mist particle generation rate in air caused by MQL was 100 to 140 times and 340 to 3300 times that under flood cooling during milling and drilling, respectively, and this ratio would be bigger at high cutting speed and metal removal rate [5]. Oil mist exposures cause many illnesses such as dermatitis, asthma, and pneumonia by skin contact and breathing [6]. Therefore, there is an urgent need for improving the cooling/lubrication and environmental performance of MQL.

Some methods applied to enhance the cooling/lubrication performance of MQL have been reported. Zhang et al. [7] developed a cryogenic minimum quantity lubrication (CMQL) system in which a small amount of lubricating oil was mixed with cryogenic air, and found that in comparison with dry condition, the application of CMQL increased tool life by 57% in end milling of Inconel 718. Su [8] studied the role of cooling/lubrication effect of CMQL in cylindrical

✉ Yu Su
suyuliu@sohu.com

¹ College of Mechanical Engineering, Jiangsu University of Science and Technology, Zhenjiang 212003, China

Fig. 1 Photographic view of electrostatic atomization milling system: 1, high-voltage electrostatic generator; 2, syringe pump; 3, cutting tool; 4, workpiece; 5, nozzle



turning of AISI H13 steel by three-dimensional finite element simulation, and proposed the development direction of CMQL. Sanchez et al. [9] proposed a new hybrid MQL-CO₂ grinding technology, that is to spray MQL oil microdroplets directly onto the grinding wheel surface and then make the oil frozen on the abrasive grains using CO₂ jet, to improve the grindability of AISI D2 tool steel. Su et al. [10] studied the application of graphite oil-based nanofluid MQL with vegetable-based oil and ester oil as base fluids in turning. It was found that graphite oil-based nanofluid MQL was more effective to reduce cutting force and cutting temperature than MQL with the corresponding base fluid, especially using LB2000 vegetable-based oil as base fluid. Itoigawa et al. [11] investigated the boundary film behavior of MQL and MQL with water (OoW) using intermittent turning process. It was reported that relative to MQL, the strength of boundary film under OoW can be sustained due to water's chilling effect. Due to the fact that the above methods for improving the cooling/lubrication performance of MQL use compressed air as atomizing driving force and droplet transport carrier, the motion of droplet is uncontrollable after being sprayed. Thus, the problem of high oil mist concentration in the working environment can't be avoided when applying them.

Installing a vacuum system or oil mist separator is commonly used to reduce the harm of oil mist to environment and human body during MQL. But it leads to the great increase in production cost. Li [12] investigated the aerosol generation rate in the air using an aerosol spectrometer during MQL in turning operation. It was found that applying higher oil flow rate in MQL brought about an increasing aerosol generation. The most effective solution to reduce the aerosol concentration in MQL process was to limit the use of lubricating oil. However, the cooling and lubricating effect of MQL is difficult to be fully played when selecting spraying conditions from environmental point of view. It has been pointed out in

Table 1 Chemical composition of Ti-6Al-4V (wt%)

| Al | V | Fe | C | O | N | H | Ti |
|------|------|------|------|------|-------|-------|---------|
| 6.43 | 4.13 | 0.15 | 0.02 | 0.14 | 0.006 | 0.001 | Balance |

reference [5] that the important source of oil mist particles in the air during the MQL is not the machining process, but the transfer of oil mist to the machining zone. Thus, the effective way of minimizing adverse environmental and worker's health effects associated with the application of MQL is to seek a controllable method to deliver mist droplets to the machining zone with less dispersion.

Electrostatic atomization is a method where the liquid is electrostatic charged and broken into fine charged droplets by means of electrical forces. Relative to pneumatic atomization, electrostatic atomization has some significant virtues such as relative ease of droplet generation, uniform distribution of droplet size, and great control of droplet transport [13–16]. So, it is expected to be a new generation of green cooling/lubrication technology in machining. Based on the principle of electrostatic atomization, Reddy et al. [17, 18] developed electrostatic lubrication (ESL) experimental setup and carried out the drilling experiments of AISI 4340 steel and SCM 440 steel under different cooling/lubrication conditions such as dry, wet, MQL and ESL with soluble oil with water, and the mixture of SAE 40 oil and micro size graphite. The results suggested that relative to dry, wet, and MQL, reduction in thrust force and tool wear and improvement of dimensional accuracy and surface roughness could be obtained with ESL. But to date, machining and environmental performance of electrostatic atomization lubrication (EAL) in milling operation has never been studied. So the objective of current study is to investigate the effects of EAL and nanofluid electrostatic atomization lubrication (NFEAL) on tool wear and environment by experiments of milling titanium alloy and oil mist concentration detection, and compare the performance with MQL.

Table 2 Mechanical properties of Ti-6Al-4V at room temperature

| Properties | Values |
|------------------------------------|--------|
| Tensile strength σ_b /MPa | 895 |
| Yield strength $\sigma_{0.2}$ /MPa | 825 |
| Elongation δ /% | 10 |
| Hardness/HRC | 34 |

Table 3 Conditions of machining experiments

| Operation | Up milling |
|--------------------------------|---|
| Milling parameters | Values |
| Cutting speed | 100 m/min |
| Feed rate | 0.1 mm/rev |
| Axial depth of cut | 2.5 mm |
| Radial depth of cut | 0.5 mm |
| Cooling/lubrication conditions | Description |
| MQL | Air pressure, 0.6 MPa; lubricant, LB2000; flow rate, 30 ml/h |
| EAL | Voltage, – 7.8 kV; lubricant, LB2000; flow rate, 30 ml/h |
| NFEAL | Voltage, – 4.5 kV; lubricant, graphite-LB2000 nanofluid; flow rate, 30 ml/h |

2 Experimental details

2.1 Machining experiments

Figure 1 shows the photographic view of electrostatic atomization milling system. It was mainly composed of high-voltage electrostatic generator (ZGY-5, Dalian Power Supply Technology Co., Ltd, China), syringe pump (LSP01-1A, Baoding Longer Precision Pump Co., Ltd, China), cutting tool, workpiece, and nozzle. The nozzle was made of stainless steel with 0.4 mm inner diameter and connected to the negative terminal of ZGY-5 high-voltage electrostatic generator, which was capable of supplying a maximum voltage of – 120 kV. LSP01-1A syringe pump was connected to the inlet of nozzle through a silicone rubber tube. The cutting tool and workpiece were connected to the ground indirectly through the machine tool.

When high-voltage electrostatic generator operated, the nozzle generated charges with the same polarity as the high-voltage supply, and opposite charges were induced on the surfaces of cutting tool and workpiece. So high-voltage electrostatic field was formed among the nozzle, cutting tool, and workpiece. When the lubrication medium passed through the nozzle, like charges were induced onto the surface of lubrication medium by conduction charging method. When the charges on the lubrication medium exceeded Rayleigh limit, the repulsive electrostatic force on the surface of charged lubrication medium overcame the surface tension and viscous force, thus making the lubrication medium breaking into tiny charged droplets. After that, the charged droplets were delivered by the electrostatic force under the electrostatic field, and attracted to the opposite charges induced on the surfaces

of cutting tool and workpiece, thus cooling and lubricating the cutting zone.

End milling experiments were performed on 100 × 100 × 100 mm Ti-6Al-4V alloy rectangular block on MVC 850 machining center by uncoated carbide inserts (model R390-11T308M-KMH13A, Sandvik Coromant). The chemical composition and mechanical properties of workpiece are given in Tables 1 and 2, respectively. The conditions of machining experiments are presented in Table 3. LB2000 biodegradable vegetable-based oil was used as lubrication medium of MQL and EAL. The MQL mists were supplied with Accu-Lube micro lubricating system through a flexible nozzle. For NFEAL application, graphite-LB2000 nanofluids were formulated by adding 0.5% by weight of 35 nm graphite nanoparticles (Beijing DK nanotechnology Co., Ltd, China) in LB2000 vegetable-based oil followed by ultrasonication (40 kHz, 100 W) for 2 h. The sedimentation experiment results show that the graphite-LB2000 nanofluids prepared were stable for more than 3 months. The dynamic viscosity, surface tension, and thermal conductivity of lubrication medium employed were measured by NDJ-9S rotational-type viscometer, BZY-1 automatic surface tension meter and TC3010L thermal conductivity measuring instrument, respectively, and the results are given in Table 4. Under all the cooling/lubrication conditions used in the current study, the nozzle was positioned towards the cutting zone with a distance of 20 mm and at an angle of 60° in relation to the cutting tool. The electrostatic atomization depends highly on the electrostatic field. Furthermore, the electrostatic field is affected by the voltage, nozzle angle, and spraying distance. Thus, the electrostatic field among the nozzle, cutting tool, and

Table 4 Physical properties of lubricant

| Properties | LB2000 | Graphite-LB2000 nanofluid (0.5 wt%) |
|-----------------------------|---------|-------------------------------------|
| Dynamic viscosity/(mpa.s) | 52 | 57 |
| Surface tension/(mN/m) | 32.2 | 29.47 |
| Thermal conductivity/(W/mK) | 0.16526 | 0.166 |

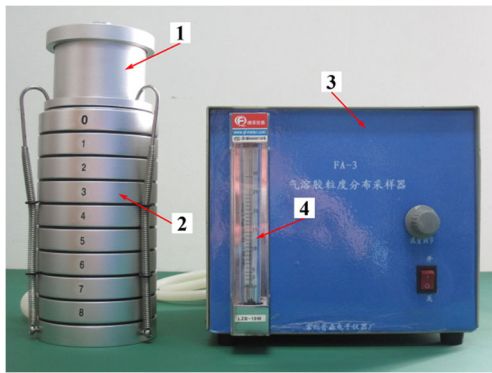


Fig. 2 FA-3 aerosol particle size distribution sampler: 1, front separator; 2, impactor; 3, main machine; 4, flowmeter

workpiece was simulated using Ansoft Maxwell under different conditions. Combined with electrostatic field simulation and preliminary experiment, the voltage, nozzle angle, and spraying distance used in EAL and NFEAL conditions were determined in order to obtain the stable atomization and deliver mist droplets towards the machining zone.

The tool wear was measured at different intervals up to 315 min of machining by means of optical digital microscope (model DSX-500, Olympus), and was examined by scanning electron microscope (SEM) equipped with energy dispersive spectroscopy (EDS).

2.2 Oil mist concentration detection experiments

2.2.1 Sampling equipment

The oil mist collection device used was a FA-3 aerosol particle size distribution sampler (Changzhou Pusen Electric Instrument Factory, China), which works based on inertial impact principle, as shown in Fig. 2. It was mainly composed of a front separator, an impactor, and a main machine with a flowmeter. The front separator was used to prevent the bounce and repeated transport of particles when sampling in the environment containing particles larger than $10\ \mu\text{m}$. The impactor consisted of nine grade aluminum discs with small orifices. A stainless steel acquisition plate and a glass fiber filter were placed under each grade disc. The particles of different sizes below $10\ \mu\text{m}$ could be captured by the impactor. The main machine was a continuously operating air extractor that could provide different sampling flow rates.

2.2.2 Calculation method of oil mist concentration

The collected oil mist was weighed with high precision FA-2004B electric analytical balance to calculate the oil mist concentration value based on gravimetric analysis method. The oil mist concentration could be calculated according to the following formula [19]

$$C = 1000 \times (M_2 - M_1) / V_0 - C_0$$

$$V_0 = q_v \times t \frac{273}{273 + K} \frac{P_0}{101324.72}$$

where C is the oil mist concentration, M_1 is the weight of filter and acquisition plate before sampling, M_2 is the weight of filter and acquisition plate after sampling, V_0 is the sampled air volume at standard state ($20\ ^\circ\text{C}$, standard atmospheric pressure), q_v is sampling flow rate, t is the sampling time, K is the ambient temperature during sampling, P_0 is the atmospheric pressure during sampling, and C_0 is the oil mist concentration of background experiment. The illustration about the background experiment was given in Section 2.2.4.

2.2.3 Sampling position and time

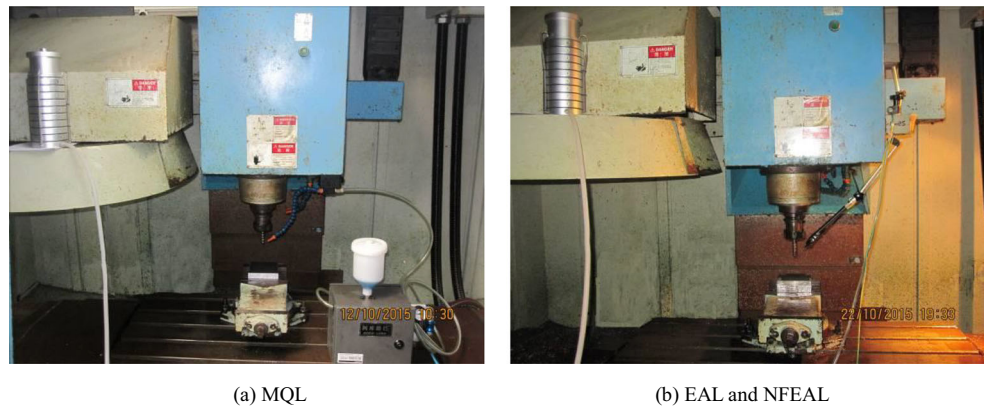
Before the oil mist was collected, the sampling position and sampling time should be considered. In order to characterize the hazard of oil mist to the worker's health, the sampling position is usually set on the operator's console outside the machine tool. However, due to the influence of some factors such as the protective door of machine tool, the size of external space, and the ambient air circulation, sampling the ambient air outside the machine tool doesn't reflect the formation of oil mist effectively. According to the requirements of oil mist concentration measurement of metal cutting machine tools in China [19], the sampling position is generally less than 1 m from the machine tool, and its height from the ground is generally the same as that of human respiratory zone. The average height of nostrils in China is about 1.5 m. Thus, in the current experiments, the sampling position was arranged in the protective door of machine tool, which was about 0.7 m away from the spindle of machine tool and 1.5 m away from the ground.

In order to enhance the oil mist sampling efficiency, the sampling flow rate was set at 28.3 L/min and the continuous sampling time was 2 h. The sampling flow rate of 28.3 L/min

Table 5 Cooling/lubrication conditions used in oil mist concentration detection

| Cooling/lubrication conditions | Description |
|--------------------------------|---|
| MQL | Air pressure, 0.6 MPa; lubricant, LB2000; flow rate, 30 ml/h |
| EAL | Voltage, $-8\ \text{kV}$; lubricant, LB2000; flow rate, 30 ml/h |
| NFEAL | Voltage, $-5, -8\ \text{kV}$; lubricant, graphite-LB2000 nanofluid; flow rate, 30 ml/h |

Fig. 3 Experimental setup of oil mist concentration detection. (a) MQL. (b) EAL and NFEAL



was within the range of 15~40 L/min specified in the measuring method of oil mist concentration of metal cutting machine tools in China [19]. And the air sampling amount for each collected sample was 3396 L, which met the sample amount standard of National Institute for Occupational Safety and Health (NIOSH) in the USA [20].

2.2.4 Experiment conditions

All the oil mist concentration detection experiments were carried out on MVC 850 machining center. During the sampling process, the protective door of machine tool was closed. In the machining process, metal dust is

generated and dispersed in the air, which interferes with the measurement of oil mist, so that the accurate oil mist concentration values can't be obtained. Therefore, when detecting the oil mist concentration, non-machining experiments were planned. And the rotational speed of cutting tool, n , was set at 0 and 1274 r/min. The cooling/lubrication conditions used in oil mist concentration detection are given in Table 5. The nozzle angle and spraying distance employed in oil mist concentration detection were the same as those in milling experiments. As a background experiment, the ambient air of laboratory was sampled before the oil mist concentration detection. Figure 3 shows the experimental setup of oil mist concentration detection.

Fig. 4 Comparison of flank wear after machining 315 min under various cooling/lubrication conditions. (a) Maximum flank wear. (b) Nose wear. (c) Notch wear at the depth of cut

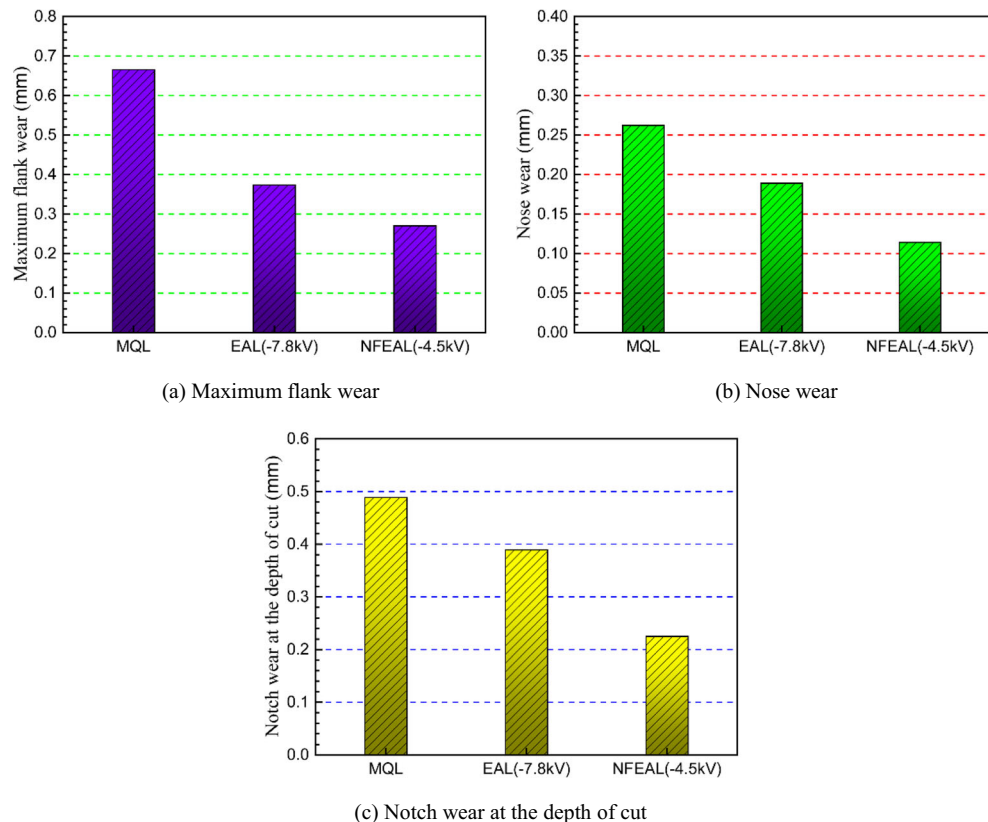
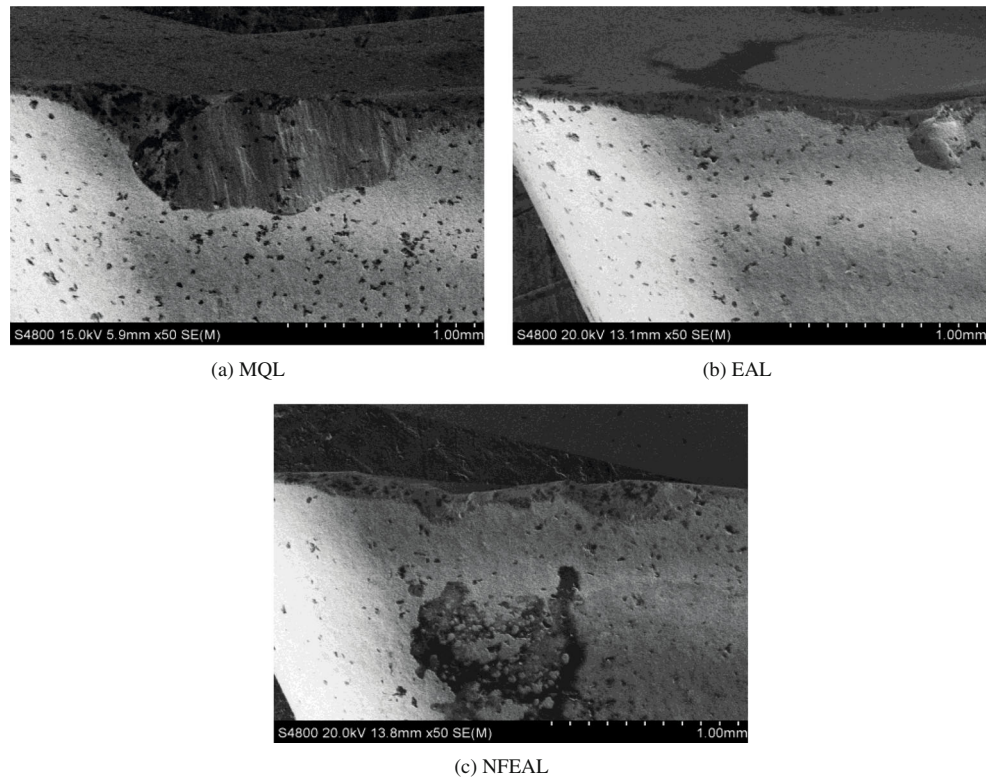


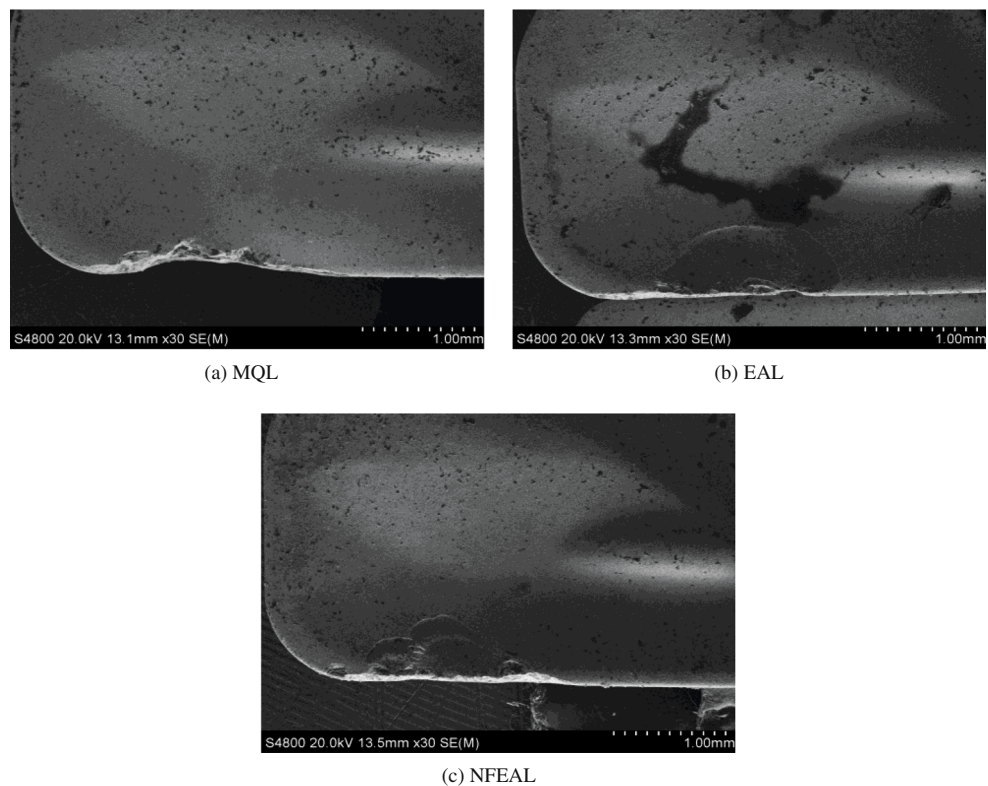
Fig. 5 SEM photos of flank faces of worn inserts after machining 315 min under various cooling/lubrication conditions. (a) MQL. (b) EAL. (c) NFEAL



According to the reference [21], when the aerodynamic diameter of oil mist particles is from 2.5 to 10 μm and less than 2.5 μm , they can enter the upper and lower respiratory tract through respiration, respectively. So the

concentrations of oil mist with aerodynamic diameter less than 10 μm (PM10) and 2.5 μm (PM2.5) were measured and calculated to evaluate the effect of cooling/lubrication conditions on the environment and worker's health.

Fig. 6 SEM photos of rake faces of worn inserts after machining 315 min under various cooling/lubrication conditions. (a) MQL. (b) EAL. (c) NFEAL



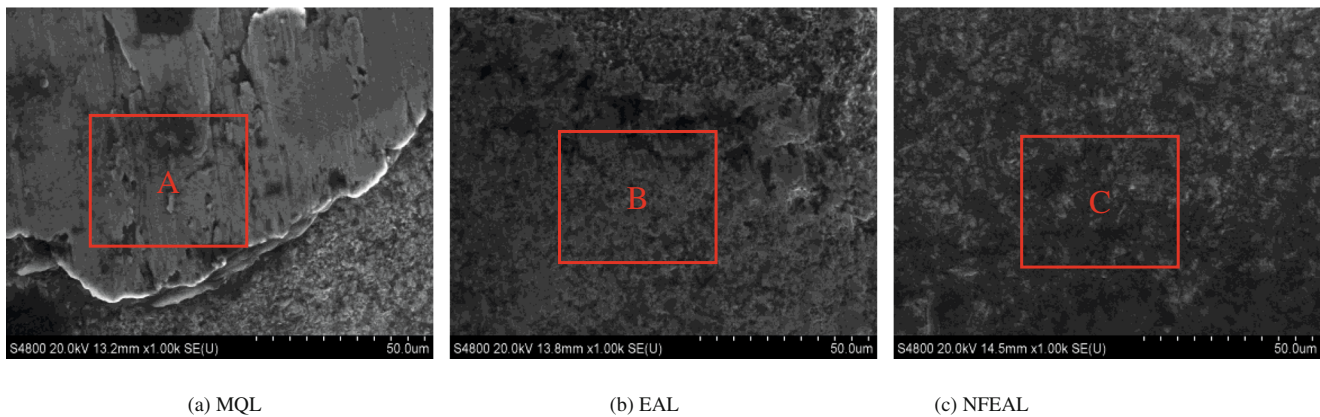


Fig. 7 SEM micrographs of flank faces of worn inserts under different cooling/lubrication conditions. (a) MQL. (b) EAL. (c) NFEAL

3 Results and discussion

3.1 Effect of cooling/lubrication conditions on tool wear

Figure 4 shows a comparison of flank wear among MQL, EAL, and NFEAL. As can be seen obviously, the cooling/lubrication conditions affected the tool wear significantly. The flank wear was in the decreasing order of MQL, EAL, and NFEAL. The reduction ratios of maximum flank wear, nose wear, and notch wear at the depth of cut in case of EAL were 43.87%, 27.78%, and 20.34%, respectively, when compared with those in case of MQL. Meanwhile, the reduction ratios of maximum flank wear, nose wear, and notch wear at the depth of cut in case of NFEAL were 59.41%, 56.40%, and 53.97%, respectively.

Figures 5 and 6 show wear morphology of rake and flank faces of worn uncoated cutting inserts after machining 315 min under various cooling/lubrication conditions, respectively. As shown in Figs. 5 and 6, the cutting inserts exhibited non-uniform flank wear, chipping, and flaking on the rake face under EAL and NFEAL conditions. However, MQL condition provided non-uniform flank wear and edge fracture wear patterns. As reported by many researchers [22–25], the temperature at the cutting edge can be above 800 °C when machining titanium alloy using carbide tool, even at moderate cutting condition. High temperature, intimate contact, and high chemical affinity between the tool and the workpiece promoted the adhesion and diffusion during the machining

of titanium alloy. Figure 7 shows the SEM micrographs of flank faces of worn inserts under different cooling/lubrication conditions. The large material adherence to the flank face was clearly observed under MQL condition (Fig. 7a). However, there was almost no obvious adhesion on flank face under EAL and NFEAL conditions (Fig. 7b, c). EDS analysis was further performed in region A, B, and C of Fig. 7 and the results are given in Table 6. High concentration of Ti in region A characterized the existence of adhered workpiece materials. Moreover, W and Co were not detected in region A, indicating that it was fully covered by adhered workpiece materials under MQL condition. Low concentration of Ti in region B and C demonstrates that there were only a very small amount of workpiece materials adhered on the flank face under EAL and NFEAL conditions. In the machining of titanium alloy, high temperature and stress coupled with the detachment of adhered workpiece materials on tool face, and the embrittlement of tool material due to diffusion of C from cutting tool to workpiece [26] accelerated the chipping, flaking and fracture of cutting tool.

Due to the close contact between the tool and the workpiece during the machining of titanium alloy, under MQL condition, mist droplets could not penetrate into the cutting interface and remove the cutting heat effectively. Under EAL and NFEAL conditions, charged mist droplets were delivered to the machining zone by electrostatic force. Owing to electrostatic hoop and Rebinder effects, charged mist droplets could enter into the cutting interface and cool/lubricate the cutting zone effectively, thus reducing

Table 6 EDS analysis of region A, B, and C in Fig. 7

| Cooling/lubrication conditions | Element wt% | | | | | | | | |
|--------------------------------|-------------|----------|----------|----------|------|----------|--------|--------|--------|
| | Titanium | Aluminum | Vanadium | Nitrogen | Iron | Tungsten | Cobalt | Carbon | Oxygen |
| MQL | 68.53 | 5.60 | 3.37 | 0.63 | 0.07 | – | – | 11.30 | 10.51 |
| EAL | 14.56 | – | – | – | – | 62.90 | 7.17 | 11.14 | 4.23 |
| NFEAL | 4.44 | – | – | – | – | 47.05 | 29.05 | 12.57 | 6.89 |



Fig. 8 SEM micrograph of thermal crack under NFEAL condition

the thermally related wear and consequently resulting in the reduction in the tool wear with EAL and NFEAL compared to MQL condition. Graphite-LB2000 nanofluid had lower surface tension and higher conductivity than LB2000 vegetable-based oil. Thus, during the electrostatic atomization process, due to the reduction of atomization resistance and the improvement of charging performance, graphite-LB2000 nanofluid tended to generate smaller droplets than LB2000 vegetable-based oil, leading to more efficient penetration of NFEAL into the cutting interface. In addition, when milling titanium alloy under NFEAL condition, graphite nanoparticles could enter into the cutting zone with charged mist droplets and help reduce the friction at the cutting interface. Thus, owing to enhanced penetration, low friction characteristic of graphite nanoparticles, and increased heat transfer capability of graphite-LB2000 nanofluids (Table 4), NFEAL presented better cooling and lubrication effect than EAL. Therefore, NFEAL was more effective than EAL in terms of reduction in tool wear.

Figure 8 shows a SEM micrograph of thermal crack under NFEAL condition. It can be seen clearly that thermal crack extended from the rake face to flank face of cutting insert, and micro-chipping happened at the cutting edge where thermal crack formed and propagated. Formation of thermal cracks reduced the strength of cutting edge. When thermal cracks propagated to a serious extent, they resulted in the catastrophic fracture of cutting edge. Although the formation and propagation of thermal cracks were accelerated by increased fluctuation of tool temperature resulting from application of cooling/lubrication conditions during intermittent milling, NFEAL did not bring about the severe tool damage (Figs. 5 and 6).

3.2 Effect of cooling/lubrication conditions on oil mist concentration

In the current experiments, the sources of oil mist generated in working environment involved the dispersion of droplets during the conveying process and the splash of droplets after hitting the cutting tool. Figure 9 shows a comparison of oil mist concentration among MQL, EAL, and NFEAL. It can be seen from Fig. 9 that whether the tool rotated or not, the oil mist concentrations of PM10 and PM2.5 were considerably less with application of EAL and NFEAL compared to MQL. Under MQL condition, mist droplets were transported to the tool by compressed air and thus the movement of droplets was not constrained. However, under EAL and NFEAL conditions, the electrostatic field was established between nozzle and cutting tool. The charged droplets were delivered towards cutting tool by means of electrical force, and got attracted to the cutting tool due to the opposite charges induced on tool face, which reduced the dispersion of droplets during the conveying process, and the splash of droplets after colliding with the cutting tool. Therefore, the oil mist concentration under EAL and NFEAL conditions was significantly lower than that

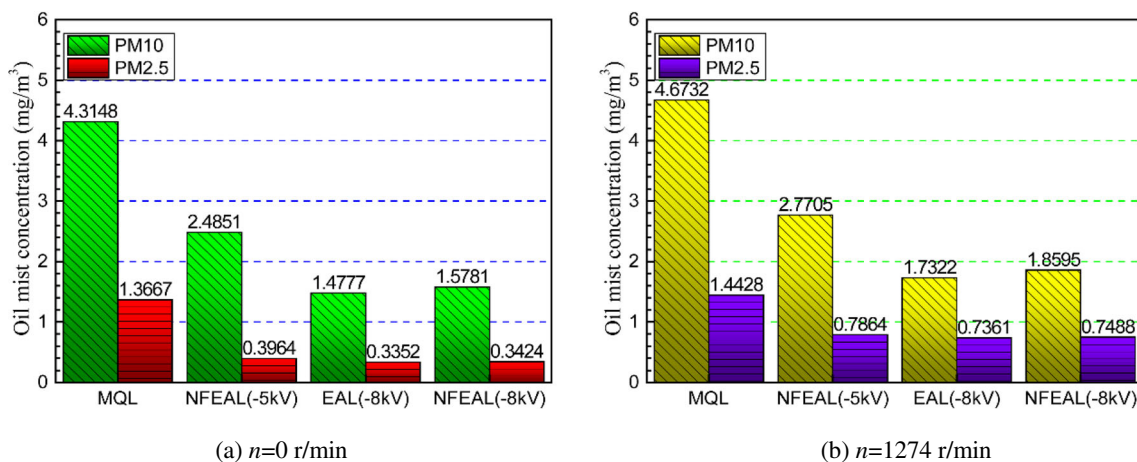


Fig. 9 Comparison of oil mist concentration under various cooling/lubrication conditions. (a) $n = 0$ r/min. (b) $n = 1274$ r/min

under MQL condition. Furthermore, NFEAL produced slightly higher oil mist concentrations of PM10 and PM2.5 than EAL. This can be attributed to the fact that fine droplets were easily formed during the NFEAL process due to the high electrical conductivity and low surface tension of graphite-LB2000 nanofluids. As shown in Fig. 9, in case of NFEAL, the oil mist concentrations of PM10 and PM2.5 decreased with the increase of voltage. This is because the increase of voltage led to an increase in the intensity of electrostatic field, which enhanced the ability of electrostatic field to control the transport process of droplets, and thus reduced the diffusion of oil mist particles into the environment, thereby resulting in a decrease in the oil mist concentration.

As can be seen clearly, regardless of cooling/lubrication conditions, the oil mist concentrations of PM10 and PM2.5 under tool rotation condition were higher than those under tool quiescence condition. The airflow field caused by tool rotation promoted the dispersion of droplets. Moreover, the droplets tended to splash after they hit the rotating tool. As a result, the oil mist concentration under tool rotation condition increased. When the tool didn't rotate, compared to MQL, NFEAL showed 42.41~63.43% and 71~74.95% reduction in the oil mist concentrations of PM10 and PM2.5, respectively. When the tool rotated at a speed of 1274 r/min, compared to MQL, NFEAL showed 40.72~60.21% and 45.49~48.10% reduction in the oil mist concentrations of PM10 and PM2.5, respectively. The percentage reduction in the oil mist concentration of PM2.5 for NFEAL relative to MQL was found to decrease significantly, as the rotational speed of cutting tool increased from 0 to 1274 r/min. The droplet velocity under NFEAL condition was lower than that under MQL condition [27]. Thus, the small size droplets under NFEAL condition were easily dispersed into the air under the action of air flow field caused by the rotation of cutting tool. This might be the reason why there was an obvious decrease in the reduction. It can be noted from Fig. 9 that whether the tool rotated or not, the oil mist concentration of PM2.5 under MQL condition far exceeded the contact limit of 0.5 mg/m³ specified by NIOSH in the USA [28]. The oil mist concentration of PM2.5 under EAL and NFEAL conditions was lower than the contact limit when the tool didn't rotate. But it was slightly higher than the contact limit when the tool rotated at a speed of 1274 r/min.

4 Conclusions

In this paper, milling experiments and oil mist concentration detection experiments were conducted under the conditions of MQL, EAL, and NFEAL. The comparative performance among MQL, EAL, and NFEAL was also analyzed. It is found that both EAL and NFEAL could reduce the tool wear significantly, but NFEAL was more effective than EAL. The oil mist concentrations of PM10 and PM2.5 for NFEAL were

less compared with those for MQL, but were a little more with respect to EAL. The oil mist concentration under NFEAL condition was found to be decreasing with the increase in voltage. So EAL and NFEAL would become a novel, promising means as an alternative to MQL because of the environmental improvement, and the reduction in tool wear and health hazard.

In further research, the influence of EAL and NFEAL process parameters such as voltage, flow rate, and type of lubricant on machining and environmental performance will be studied detailedly by experiments to optimize the EAL and NFEAL machining process.

Funding information The authors received financial support of this research from National Natural Science Foundation of China under contract no. 51205177, Natural Science Foundation of Jiangsu Province under contract nos. BK2012277 and BK20171307, Natural Science Program for Basic Research of Jiangsu Province under contract no. 08KJB460002, and Research Fund of DML-HYIT (HGDML-0901).

References

1. Sharma AK, Tiwari AK, Dixit AR (2016) Effects of minimum quantity lubrication (MQL) in machining processes using conventional and nanofluid based cutting fluids: a comprehensive review. *J Clean Prod* 127:1–18
2. Liu ZQ, Chen M, An QL (2015) Investigation of friction in end-milling of Ti-6Al-4V under different green cutting conditions. *Int J Adv Manuf Technol* 78:1181–1192
3. Sharif MN, Pervaiz S, Deiab I (2017) Potential of alternative lubrication strategies for metal cutting processes: a review. *Int J Adv Manuf Technol* 89(5-8):1–33
4. Chetan GS, Venkateswara Rao P (2015) Application of sustainable techniques in metal cutting for enhanced machinability: a review. *J Clean Prod* 100:17–34
5. Li XL, He N, Li L (2005) MQL technology in green cutting. *Aviat Precis Manuf Technol* 41(2):24–35
6. Chen MR, Tsai P, Chang C, Shih T, Lee W, Liao PC (2007) Particle size distribution of oil mists in workplace atmospheres and their exposure concentrations to workers in a fastener manufacturing industry. *J Hazard Mater* 146:393–398
7. Zhang S, Li JF, Wang YW (2012) Tool life and cutting forces in end milling Inconel 718 under dry and minimum quantity cooling lubrication cutting conditions. *J Clean Prod* 32:81–87
8. Su Y (2016) Investigation into the role of cooling/lubrication effect of cryogenic minimum quantity lubrication in machining of AISI H13 steel by three-dimensional finite element method. *Proc Inst Mech Eng B: J Eng Manuf* 230(6):1003–1016
9. Sanchez JA, Pombo I, Alberdi R, Izquierdo B, Ortega N, Plaza S, Martinez-Toledano J (2010) Machining evaluation of a hybrid MQL-CO₂ grinding technology. *J Clean Prod* 18:1840–1849
10. Su Y, Gong L, Li B, Liu ZQ, Chen DD (2016) Performance evaluation of nanofluid MQL with vegetable-based oil and ester oil as base fluids in turning. *Int J Adv Manuf Technol* 83:2083–2089
11. Itoigawa F, Childs THC, Nakamura T, Belluco W (2006) Effects and mechanisms in minimal quantity lubrication machining of an aluminum alloy. *Wear* 260:339–344
12. Li KM (2006) Predictive modeling of near dry machining: mechanical performance and environmental impact. Ph.D. thesis, Georgia Institute of Technology, United States

13. Watanabe H, Matsuyama T, Yamamoto H (2003) Experimental study on electrostatic atomization of highly viscous liquids. *J Electrostat* 57(2):183–197
14. Jaworek A, Sobczyk AT (2008) Electrospraying route to nanotechnology: an overview. *J Electrostat* 66(3–4):197–219
15. Maski D, Durairaj D (2010) Effects of electrode voltage, liquid flow rate, and liquid properties on spray chargeability of an air-assisted electrostatic-induction spray-charging system. *J Electrostat* 68(2):152–158
16. Su Y, Tang ZC, Wan RR (2017) An investigation on the electrostatic atomization mode of nanofluid using cutting tool as electrode. *Adv Mech Eng* 9(11):1–12
17. Reddy NSK, Yang M (2010) Development of an electro static lubrication system for drilling of SCM 440 steel. *Proc Inst Mech Eng B: J Eng Manuf* 224(2):217–224
18. Reddy NSK, Nouari M, Yang M (2010) Development of electrostatic solid lubricant system for improvement in machining process performance. *Int J Mach Tools Manuf* 50(9):789–797
19. National Metal Cutting Machine Standardization Technical Committee (2009) Method for measuring oil mist concentration of metal cutting machine tools (GB/T 23574–2009). China Standard Press, Beijing
20. NIOSH Metal Working Fluids: Method 5524, Issue 1, 2003. In: Eller PM, Cassinelli ME (eds) NIOSH Manual of Analytical Methods (NMAM), 4th edn. National Institute for Occupational Safety and Health, DHHS (NIOSH) Publication No, Cincinnati, pp 94–113
21. U.S. Environmental Protection Agency (2008) Integrated Review Plan for the National Ambient Quality Standards for Particulate Matter. Research Triangle Park, North Carolina
22. Su Y, He N, Li L, Li XL (2006) An experimental investigation of effects of cooling/lubrication conditions on tool wear in high-speed end milling of Ti-6Al-4V. *Wear* 261(7–8):760–766
23. Zhang XQ, Yamazaki K, Yamaguchi Y (2002) A study on a novel tool temperature measurement method in high-speed machining of titanium. Proceedings of the 17th Annual Meeting of the American Society for Precision Engineering, St. Louis, MO, pp.425–428
24. Hong SY, Ding Y (2001) Cooling approaches and cutting temperatures in cryogenic machining of Ti-6Al-4V. *Int J Mach Tools Manuf* 41(10):1417–1437
25. Mao C, Zhang YC, Peng XX, Zhang B, Hu YL, Bi ZM (2018) Wear mechanism of single cBN-WC-10Co fiber cutter in machining of Ti-6Al-4V alloy. *J Mater Process Technol* 259:45–57
26. Wang M, Zhang YZ (1986) Diffusion wear in milling titanium alloys. *Mater Sci Technol* 4:548–553
27. Cao H (2015) Development of nanofluid electrostatic atomization device for green cutting and its atomization characteristic test. Master thesis, Jiangsu University of Science and Technology, China
28. National Institute for Occupational Safety and Health (NIOSH), Recommendation for a metalworking fluids standard, <http://www.cdc.gov/NIOSH/> (Chapter 1). Accessed 6 June 2014

Publisher's note Springer Nature remains neutral with regard to jurisdictional claims in published maps and institutional affiliations.